

In Vitro Demonstration of Human Lipoyl Synthase Catalytic Activity in the Presence of NFU1

Douglas M. Warui, Debangsu Sil, Kyung-Hoon Lee, Syam Sundar Neti, Olga A. Esakova, Hayley L. Knox, Carsten Krebs,* and Squire J. Booker*



Cite This: *ACS Bio Med Chem Au* 2022, 2, 456–468



Read Online

ACCESS |



Metrics & More



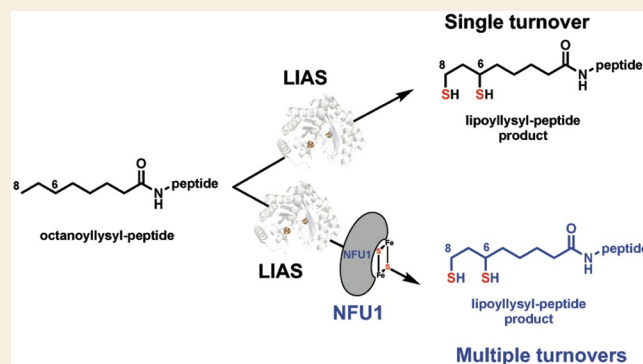
Article Recommendations



Supporting Information

ABSTRACT: Lipoyl synthase (LS) catalyzes the last step in the biosynthesis of the lipoyl cofactor, which is the attachment of sulfur atoms at C6 and C8 of an *n*-octanoyllysyl side chain of a lipoyl carrier protein (LCP). The protein is a member of the radical *S*-adenosylmethionine (SAM) superfamily of enzymes, which use SAM as a precursor to a 5'-deoxyadenosyl 5'-radical (5'-dA \cdot). The role of the 5'-dA \cdot in the LS reaction is to abstract hydrogen atoms from C6 and C8 of the octanoyl moiety of the substrate to initiate subsequent sulfur attachment. All radical SAM enzymes have at least one [4Fe–4S] cluster that is used in the reductive cleavage of SAM to generate the 5'-dA \cdot ; however, LSs contain an additional auxiliary [4Fe–4S] cluster from which sulfur atoms are extracted during turnover, leading to degradation of the cluster. Therefore, these enzymes catalyze only 1 turnover in the absence of a system that restores the auxiliary cluster. In *Escherichia coli*, the auxiliary cluster of LS can be regenerated by the iron–sulfur (Fe–S) cluster carrier protein NfuA as fast as catalysis takes place, and less efficiently by IscU. NFU1 is the human ortholog of *E. coli* NfuA and has been shown to interact directly with human LS (i.e., LIAS) in yeast two-hybrid analyses. Herein, we show that NFU1 and LIAS form a tight complex in vitro and that NFU1 can efficiently restore the auxiliary cluster of LIAS during turnover. We also show that BOLA3, previously identified as being critical in the biosynthesis of the lipoyl cofactor in humans and *Saccharomyces cerevisiae*, has no direct effect on Fe–S cluster transfer from NFU1 or GLRX5 to LIAS. Further, we show that ISCA1 and ISCA2 can enhance LIAS turnover, but only slightly.

KEYWORDS: liponic acid, *S*-adenosylmethionine, iron–sulfur clusters, NFU1, multiple mitochondrial dysfunctions syndrome, radical SAM, lipoyl synthase, LIAS



INTRODUCTION

Lipoic acid is an eight-carbon straight-chain fatty acid containing sulfur atoms at C6 and C8.^{1–3} It is found in all domains of life.^{4–11} Its primary cellular function is as a cofactor in several multienzyme complexes that are involved in energy metabolism and the catabolism of certain amino acids.^{7,11} In humans, these complexes include the pyruvate dehydrogenase complex (PDC), the α -ketoglutarate dehydrogenase complex (KGC), the branched chain oxo-acid dehydrogenase complex (BCODC), the glycine cleavage system (GCS), and the α -ketoacidipate complex (KAC), all of which are found in the mitochondrion.^{12,13} In each of these complexes, lipoic acid is tethered covalently in an amide linkage to a target lysyl residue of a lipoyl carrier protein (LCP), producing a 14 Å flexible appendage that can access active sites of other component proteins. Very little free lipoic acid exists in the cell in the absence of supplementation. In fact, the molecule is biosynthesized in its cofactor form rather than as the free acid. This biosynthetic pathway involves a bacterial-type acyl carrier protein (ACP) upon which the C8 fatty acyl backbone

is constructed. In humans, LIPT2, an octanoyltransferase, is believed to transfer the octanoyl chain from octanoyl–ACP to the target lysyl residue only of the H protein, the LCP of the GCS. Next, lipoyl synthase (LS, LIAS in humans and LipA in *Escherichia coli*) attaches thiol groups at C6 first, and then at C8, to give the intact lipoyl cofactor.^{13,14} Finally, LIPT1, a lipoyltransferase, is believed to distribute the lipoyl appendage to other LCPs^{13,15} (Figure 1). This biosynthetic pathway differs from the canonical pathway in *E. coli* wherein octanoyltransferase transfers an octanoyl group directly to each of the LCPs, which include the H protein of the GCS and the E2 subunits of the KGC and PDC.^{16–21} LipA then acts on

Received: March 20, 2022

Revised: May 20, 2022

Accepted: May 20, 2022

Published: June 13, 2022



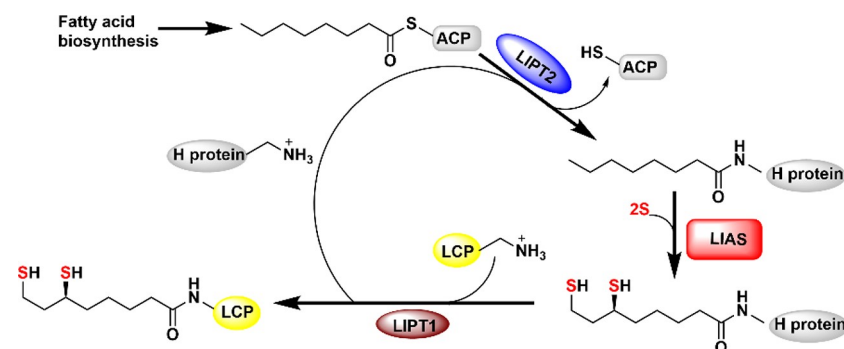


Figure 1. Proposed de novo biosynthetic scheme of lipoyl cofactor in humans.

P60716	1	MS	-----	KP I	-----	VMERGVKYRD	-----	ADKMALIPVK	NVATEREALLR	36		
Q8DLC2	1	MALS	-----	RPL	-----					7		
O43766	1	MSLRCGDAARTLGRVFGRYFCSPVRPLSLPDKKKELLQNGPDLQDFVSGDLADRSTWDEYKGNLKRQKGERLR								75		
PQWK91	1	MSVAEE	-----		-----			GRLLLRLEVR	NAQTPIE	24		
P60716	37	KPEWMKIKLPADSTRIQGIKAAAMRKNGLHSV	EEAS	CPNLAEC	FNHG	-----	TATFMILGAI	CTRR	CPFC	DVAHG	106	
Q8DLC2	8	PSWLRKPLGK	ASEISTVQRLVRQYGIHTI	CEEGRC	PNRGE	CYGGQK	-----	TATFLLLGPT	CTRA	CAF	CQVEKG	75
O43766	76	LPPWLKTEIPM	GKNYNKLNKTLRNLNLHTV	EEAR	CPNIGE	CWGGGEYATATAT	IMLMGDT	CTRG	CRFC	SVKTA	149	
PQWK91	25	KPPWIKTRARI	GPEYTELKNLVRREGLHTV	EEAG	CPNIFE	CWEDR	-----	EATFLIGGDQ	CTRR	DFC	QIDTG	93
P60716	107	R	PVAPDANEPVKLAQTIADMALRYVIVTSVDRDDL	RDGGAQH	FADCITAI	REKSPQIKIETLVPDFRGRMDR					178	
Q8DLC2	76	HAPAAVDPEEPTKIAAAVATLGLRYVVLTSVARDDL	PDQAGQFVATMAAIRQRCPGTE	IEVLS	PDFRMDRGRLS						150	
O43766	150	RNPPPLDASEPYNTAKAIAEWGLDYVVLTSVDRDD	MPDGGAEHIAKTVSYLKERNPKILVECLT	PDFR	GGDL	K					221	
PQWK91	94	K	PAELDRDEPRRADSVRTMGLRYATVTGVARD	DLPDGGAWLYAATVRAIKELNPSTGV	VELLIPDFN	GEPT					165	
P60716	179		ALDILTATPPDVFNHNLENVPRIYRQVR	PGADYNWSL	KLLERFKEA	HEIPTKSGLMVGLGETNEE	IEVM				249	
Q8DLC2	151	QRDCIAQIVAAQPACYNHNLETVRR	LQGPVR	RGATYES	SLRVLATVKELNPD	IPKSGLMGLGETEAE	IIETL				224	
O43766	222		AIEKVALSGLDVYAHNVETVPELQSKVRD	PANFDQSLRVLKHA	KKVQPDV	ISKTSIMLGLGENDEQVYATM					293	
PQWK91	166		LAEVFESGPEVLAHNVETVPRIFKRIR	PAFTYRRSL	GLVLTAA	DAGLVTKSNLILGLGETS	DEVRTAL				233	
P60716	250	RDLRRHGVTMLTLGQYLQPSRHHL	PVQRYVSPDEFDEMKA	EALAMGFTHAAC	CGPFVRS	SYHA	-----			DLQ	314	
Q8DLC2	225	KDLRRVGC	DRLTLGQYLP	PSLSHLPVVKY	WTPEEFNTLGN	IARELGFSHVRS	SGPLVRS	SYHAAEGG	-----		290	
O43766	294	KALREADV	CDLTLGQYMQP	TRRH	LKVEEYITPEKFKY	WEKVGNELGFHYTAS	GPLVRS	SYKAGEFFL	KNLVAKRK		368	
PQWK91	234	GDLRDAGCD	IVITIQYLR	PSARHHP	VERWVKPEEFVQ	FARFAEGLGFAGVLAGPLVRS	SYRAGR	LYEQ	-----	ARN	304	
P60716	315	AKGMEVK									321	
Q8DLC2												
O43766	369	TKDL									372	
PQWK91	305	SRALASR									311	

Figure 2. Sequence alignment of LS proteins from *E. coli* (P60716), *M. tuberculosis* (P9WK91), *T. elongatus* (Q8DLC2), and humans (O43766). The conserved residues that ligate the auxiliary and the RS clusters of LS are highlighted in blue and red, respectively.

each of the octanoyllysyl-LCPs to generate the respective lipoyl cofactor.^{22–24}

LS belongs to the radical *S*-adenosylmethionine (SAM) superfamily of enzymes, which use a [4Fe–4S] cluster cofactor to cleave SAM reductively to produce a 5′-deoxyadenosyl 5′-radical (5′-dA•).^{24–33} In LS catalysis, the 5′-dA• is used to abstract hydrogen atoms (H•) from C6, and then from C8, of the octanoyllysyl residue to allow for sulfur attachment.^{34–37} Unlike most radical SAM (RS) enzymes, which contain only one [4Fe–4S] cluster, LS contains two [4Fe–4S] clusters.^{34,38–40} One cluster, termed the RS cluster, is found in all RS enzymes and is ligated by three cysteine residues in a conserved CxxxCxxC motif. SAM binds to the unligated iron ion of this cluster, which is a prerequisite for its reductive cleavage.^{27,41–43} The second cluster, termed the auxiliary cluster, is bound by cysteines in an N-terminal CxxxxCxxxxC motif and a C-terminal serine in a conserved RSSY motif (Figure 2). This cluster has been shown to be the source of the appended sulfur atoms, resulting in its degradation as a result of turnover.^{36,44,45} Therefore, LS catalyzes no more than 1

turnover during *in vitro* reactions in the absence of a system that restores the auxiliary [4Fe–4S] cluster.^{46,47}

Recently, it was shown that the iron–sulfur (Fe–S) cluster carrier protein *E. coli* NfuA can efficiently regenerate the auxiliary [4Fe–4S] cluster of *E. coli* LipA, permitting LipA to perform multiple turnovers.^{46,47} Fe–S cluster assembly and repair is a highly regulated process that is coordinated by a complex network of proteins. In bacteria, yeast, and human model systems, de novo biogenesis of Fe–S clusters involves transient assembly of clusters on the scaffold protein ISCU (IscU in bacteria), with their subsequent transfer directly to recipient apo acceptor proteins or to a subset of late-acting carrier proteins.^{48–55} Among others, mitochondrial proteins BOLA3, ISCA1, ISCA2, GLRX5, and NFU1 have been implicated in Fe–S cluster assembly and trafficking in humans.^{52,56–58} Select mutations in genes encoding these proteins have been reported to be pathogenic and to cause severe infantile disorders of systemic energy metabolism and multiple mitochondrial dysfunctions syndrome types 1–5 (MMDS).^{48,59,60} Some of the severe manifestations of MMDS include weakness, respiratory failure, lack of neurologic

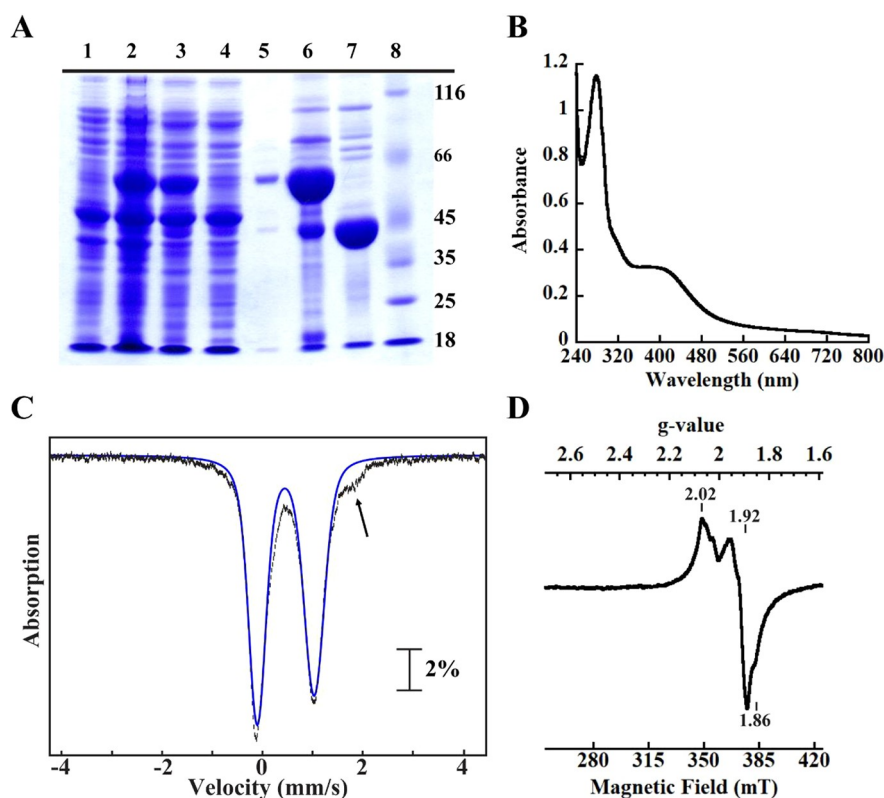


Figure 3. Biophysical characterization of LIAS: SDS–PAGE gel analysis of the expression and purification of LIAS on a Ni–NTA column (A), UV–vis scan of LIAS (B), Mössbauer spectrum of LIAS (C), and EPR spectrum of dithionite-reduced LIAS (D). (A) Lane 1, pre-IPTG induction; lane 2, post-IPTG induction; lane 3, crude lysate; lane 4, Ni–NTA column flow-through; lane 5, wash; lane 6, SUMO–LIAS fusion eluate; lane 7, LIAS after the SUMO tag is removed; lane 8, protein molecular weight ladder. (B) The UV–vis absorption scan of 8 μM purified LIAS showing a broad absorption at ~ 410 nm, which is typical for proteins that bind $[\text{4Fe–4S}]$ clusters. (C) The Mössbauer spectrum of 380 μM LIAS at 4.2 K, collected in the presence of a 53 mT external magnetic field applied parallel to the direction of propagation of the γ beam. The vertical bars represent the experimental spectrum, and the blue line shows the features associated with a $[\text{4Fe–4S}]^{2+}$ cluster. The arrow indicates the shoulder resulting from spectral features of a site-differentiated $[\text{4Fe–4S}]^{2+}$ cluster. (D) The EPR spectrum of 400 μM LIAS reduced with 4 mM dithionite and collected at 10 K with 10 mW microwave power and 0.2 mT modulation amplitude confirming bound $[\text{4Fe–4S}]$ clusters.

development, hyperglycemia, lactic acidosis, and early death,^{61–64} symptoms associated with defective lipoic acid biosynthesis. Biochemical features of patients with pathogenic mutations in genes encoding these proteins include decreased activities of several mitochondrial Fe–S cluster-containing enzymes, including complex-I, complex-II, and LIAS.⁶⁵ These studies suggest that BOLA3, ISCA1, ISCA2, GLRX5, and NFU1 may play important roles in Fe–S cluster biogenesis, trafficking, and regeneration mechanisms, especially for LIAS. However, exactly how these proteins function remains elusive.

To date, our understanding of the mechanism of lipoyl cofactor formation is derived mainly from in vivo and in vitro studies of the *E. coli* enzyme,^{10,24,34,36,37,39,66–69} with additional insight from studies of enzymes from *Sulfolobus solfataricus*,⁷⁰ *Thermosynechococcus elongatus*,⁴⁴ and *Mycobacterium tuberculosis*.^{71,72} Only recently has human LIAS been isolated and investigated in vitro. In one study, LIAS was used to show how paramagnetic NMR can be leveraged to demonstrate SAM and substrate binding to RS enzymes.⁷³ In a second study, the effect of ISCA2 and ISCU [among other iron sulfur cluster (ISC) assembly proteins] on the de novo in vitro reconstitution of the Fe–S clusters on LIAS was assessed.⁷⁴ However, neither study determined LIAS activity quantitatively nor specifically addressed how the auxiliary cluster of LIAS is restored during turnover. The lack of robust in vitro biochemical studies on LIAS, and particularly how the

implicated Fe–S cluster trafficking proteins BOLA3, ISCA1, ISCA2, GLRX5, and NFU1 function in lipoyl cofactor biosynthesis, led us to investigate how the auxiliary cluster of LIAS is regenerated after turnover.

Herein, we show that NFU1 and LIAS form a tight complex in vitro, as has been shown in in vivo yeast two-hybrid studies,⁷⁵ and that NFU1 can efficiently restore the auxiliary cluster of LIAS during turnover. We also investigate several additional Fe–S cluster carrier proteins, including BOLA3, previously identified as being critical in the biosynthesis of the lipoyl cofactor in humans and *Saccharomyces cerevisiae*. However, our in vitro studies suggest that BOLA3 has no direct effect on Fe–S cluster transfer from NFU1 or GLRX5 to LIAS. Further, we show that ISCA1 and ISCA2 can enhance LIAS turnover, but only slightly.

RESULTS

Isolation and Characterization of LIAS

Full-length human LIAS (UniProtKB O43766) is composed of 372 amino acids; however, there are several predicted isoforms of shorter length. Importantly, the first 27 amino acids are predicted to form the mitochondrial targeting sequence. When we attempted to express this full-length construct, almost all the protein was produced in inclusion bodies. Similar to two recent publications,^{73,74} we therefore engineered a construct

P63020	1	MIRIS	-----DAAQAHF	AK	14		
Q9UMS0	1	MAATARRGWGAAVAAGLRRRF	CHMLKNPYTIKKQPLHQFVQRPLFPLPAAFYHP	VR	57		
P63020	15	LLANQEEGT	-QIRVFINPGT	PNAECGVS	YCPPDA-----VEATDT	54	
Q9UMS0	58	YMF	IQTQDTPNPNSLKFIPGKPVLETRTMDFFTPAAAFRSPLARQLFRIEGVKS	VFF	114		
P63020	55	ALKFDLLTAYVDELSAPYLEDAE	IDFVTDQLGSQLTL	---KAPNAKMRKVADDA	PLM	108	
Q9UMS0	115	GPDFITVTKENEELDWNLLKPD	IYATIMDFFASGLPLVTEETPSGEAGSEEDDE	-VV	170		
P63020	109	ERVEYMLQSQINPQLAGHGGRVSLME	ITEDGYAILQFGGG	CNGC	SMVDVTLKEGIEK	165	
Q9UMS0	171	AMIKELLDTRIRPTVQEDGGDV	-IYKGFEDGIVQLKLQGS	C	TSC	CPSSIIITLKNGIQN	226
P63020	166	QLLNEFP	ELKGV	RDLETHQRGEHS	YY	191	
Q9UMS0	227	MLQFYI	PEVEGVEQVMDD	ESDEKEANS	P	254	

Figure 4. Amino acid sequence alignment of *E. coli* NfuA (P63020) and human NFU1 (Q9UMS0) showing the two conserved cysteine residues that ligate the Fe–S cluster highlighted in red.

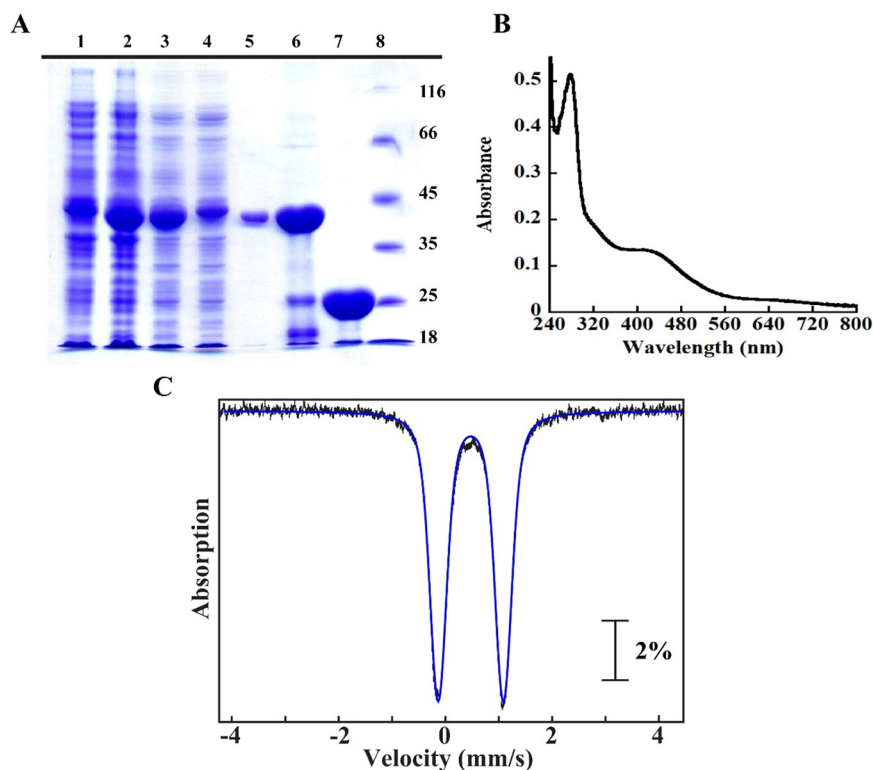


Figure 5. SDS–PAGE analysis of the expression and purification of NFU1 on a Ni–NTA column (A), UV–vis scan of 15 μM NFU1 (B), and Mössbauer spectra of NFU1 (C). (A) Lane 1, pre-IPTG induction; lane 2, post-IPTG induction; lane 3, crude lysate; lane 4, Ni–NTA column flow-through; lane 5, wash; lane 6, SUMO–NFU1 fusion eluate; lane 7, NFU1 after the SUMO tag is removed; lane 8, protein molecular weight ladder. (B) The UV–vis absorption scan spectrum of 15 μM purified NFU1 showing a broad absorption at ~ 410 nm indicative of a bound [4Fe–4S] cluster. (C) The 4.2 K Mössbauer spectra of 860 μM NFU1 in the presence of a 53 mT external magnetic field applied parallel to the direction of propagation of the γ beam. The vertical bars represent the experimental spectra, and the blue line shows the features associated with a [4Fe–4S] $^{2+}$ cluster.

(amino acids 28–372) that lacked the mitochondrial targeting sequence, which expressed well in *E. coli* and was amenable to purification with its two [4Fe–4S] cluster cofactors largely intact. This protein contained an N-terminal SUMO tag, which was removed after purification, affording an LIAS variant containing a Gly–His N-terminal appendage. The LIAS gene was expressed along with genes on plasmid pDB1282, which harbors the *Azotobacter vinelandii* *isc* operon.⁷⁶ This coexpression strategy has been shown to enhance the production of soluble *E. coli* LipA as well as its Fe–S cluster content.³⁴ The protein was purified under anoxic conditions using Ni–NTA

immobilized metal affinity chromatography (Ni–IMAC) followed by size-exclusion chromatography (SEC) to remove impurities such as protein aggregates and unbound iron and sulfide species. Upon purification, the protein was found to be $\geq 95\%$ homogeneous (Figure 3A) and contained 9.5 ± 0.1 iron and 5.5 ± 0.1 sulfide ions per polypeptide after accounting for a correction factor of 1.6 for the Bradford method of protein quantification, which was established by quantitative amino acid analysis. The UV–vis spectrum (Figure 3B) showed a broad absorption feature at ~ 410 nm typical of [4Fe–4S] cluster binding proteins. The 4.2 K/53 mT Mössbauer

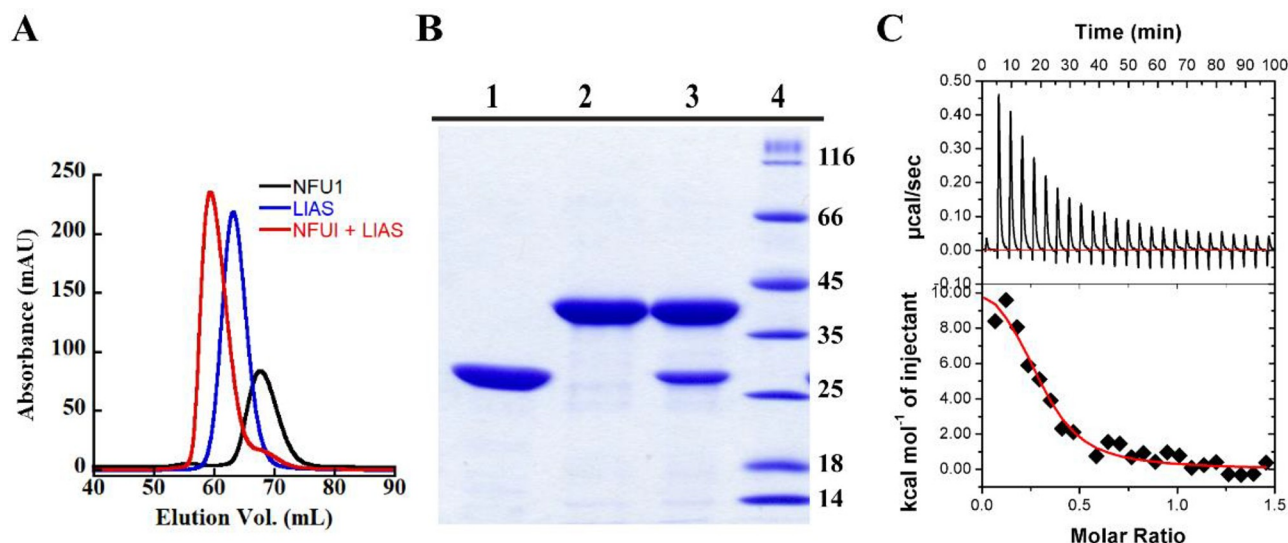


Figure 6. Size-exclusion gel filtration chromatography elution profiles of holo-LIAS (100 μM, blue), holo-NFU1 (200 μM, black), and a 1:1 mixture of holo-LIAS and holo-NFU1 (100 μM each, red) (A). SDS-PAGE analysis of the chromatographed proteins: lane 1, holo-NFU1 alone; lane 2, holo-LIAS alone; lane 3, a mixture of holo-NFU1 and holo-LIAS, indicating complex formation (B). ITC binding results of LIAS titrated into NFU1, showing entropically driven binding with a dissociation constant (K_D) of $0.7 \pm 0.2 \mu\text{M}$ (C).

spectrum of LIAS (Figure 3C) is dominated by a quadrupole doublet with parameters [isomer shift (δ) = 0.46 mm/s, quadrupole splitting (ΔE_Q) = 1.14 mm/s; ~87% of total intensity, 1.7 equiv of [4Fe-4S] per LIAS, blue line] typical of [4Fe-4S]²⁺ clusters.⁷⁷ The shoulder indicated by the arrow is at a position typically observed for the “Fe(II)-like” site of a site-differentiated [4Fe-4S]²⁺ cluster.³⁶ Analysis of the field dependence of spectra collected in a 53 mT magnetic field and zero field (Figure S1) suggests the presence of ~0.3 equiv of [3Fe-4S]⁰ cluster. The electron paramagnetic resonance (EPR) spectrum of purified LIAS after reduction with dithionite and recorded at 10 K (Figure 3D) shows a rhombic signal typical of [4Fe-4S]⁺ clusters, with estimated g -values of 2.02, 1.92, and 1.86. The UV-vis, Mössbauer, and EPR spectra in concert with iron and sulfide quantification are consistent with the presence of two [4Fe-4S]²⁺ clusters, as has been shown previously for human LIAS⁷⁴ and the *E. coli*,³⁴ *M. tuberculosis*,^{71,72} and *T. elongatus* enzymes.⁴⁴ It should be noted that our iron quantification shows 1.5 irons beyond the eight that our model suggests and that this additional iron is not observed in the Mössbauer spectrum. We believe that the discrepancy is due to systematic inaccuracies in iron and protein quantification.

Isolation and Characterization of NFU1

In a recent *in vitro* study, *E. coli* NfuA was shown to regenerate the auxiliary cluster of *E. coli* LipA after each turnover, thus allowing LipA to act catalytically.⁴⁷ There have also been several recent *in vitro* studies of NFU1, the human ortholog of *E. coli* NfuA. In one study, focused on NMR solution structures of NFU1, it was shown that holo-NFU1 could donate its [4Fe-4S] cluster to apo aconitase,⁷⁸ while in another, holo-NFU1 was reported to transfer a [2Fe-2S] cluster to apo ferredoxin 1 and ferredoxin 2.⁷⁹ Given the effects of *E. coli* NfuA on *E. coli* LipA turnover and the activation of aconitase by NFU1, we assessed the effect of NFU1 on LIAS turnover. Like NfuA, NFU1 is bimodular, with a degenerate N-terminal A-type domain and a highly conserved NifU-like C-terminal Fe-S cluster binding domain. Two cysteine residues in a

conserved C-terminal CxxC motif are believed to serve as ligands to a [4Fe-4S] formed at the interface of two monomers both in NfuA and in NFU1 (Figure 4), although there have been disagreements in the literature concerning whether this form is biochemically relevant or whether a form containing a [2Fe-2S] cluster is more relevant.^{64,80}

To study the effect of NFU1 on LIAS activity, we first expressed and purified the full-length construct (amino acids 1–254) and a construct lacking the mitochondrial transit sequence (amino acids 10–254). Unfortunately, both constructs led to poorly behaved protein products that existed mostly in higher order oligomeric states that were difficult to resolve by SEC. We therefore tried a shorter N-terminally truncated variant (amino acids 59–254). The region that was removed is predicted by AlphaFold⁸¹ (AF-Q9UMS0-F1) to be highly unstructured, while the truncated variant is well-structured and has been reported in previous studies.^{78,82} The construct was overproduced in the presence of plasmid pDB1282 and expressed as a fusion with an N-terminal SUMO tag that was removed during purification to yield NFU1 containing a Gly-His N-terminal appendage. The protein was isolated under anoxic conditions using Ni-IMAC followed by SEC and shown to be ≥95% homogeneous by sodium dodecyl sulfate-polyacrylamide gel electrophoresis (SDS-PAGE) gel analysis (Figure 5A). The UV-vis spectrum of the protein, with a distinctive feature at 410 nm, is consistent with the presence of a [4Fe-4S] cluster (Figure 5B), as has been observed in previous studies.⁷⁵ Analysis of ⁵⁷Fe-labeled NFU1 by Mössbauer spectroscopy (Figure 5C) reveals that the spectrum is dominated by a single quadrupole doublet (δ = 0.48 mm/s, ΔE_Q = 1.20 mm/s; ~97% of total intensity, blue line) typical of [4Fe-4S]²⁺ clusters.⁷⁷ When NFU1 was analyzed by EPR, a very weak signal was observed with and without dithionite reduction (Figure S2), suggesting that the [4Fe-4S] cluster is not easily reduced to the [4Fe-4S]⁺ state. Iron and sulfide analysis indicated that the isolated protein contained 2.40 ± 0.02 irons and 3.00 ± 0.03 sulfides per polypeptide, consistent with a bridging [4Fe-4S] cluster between two NFU1 monomers.

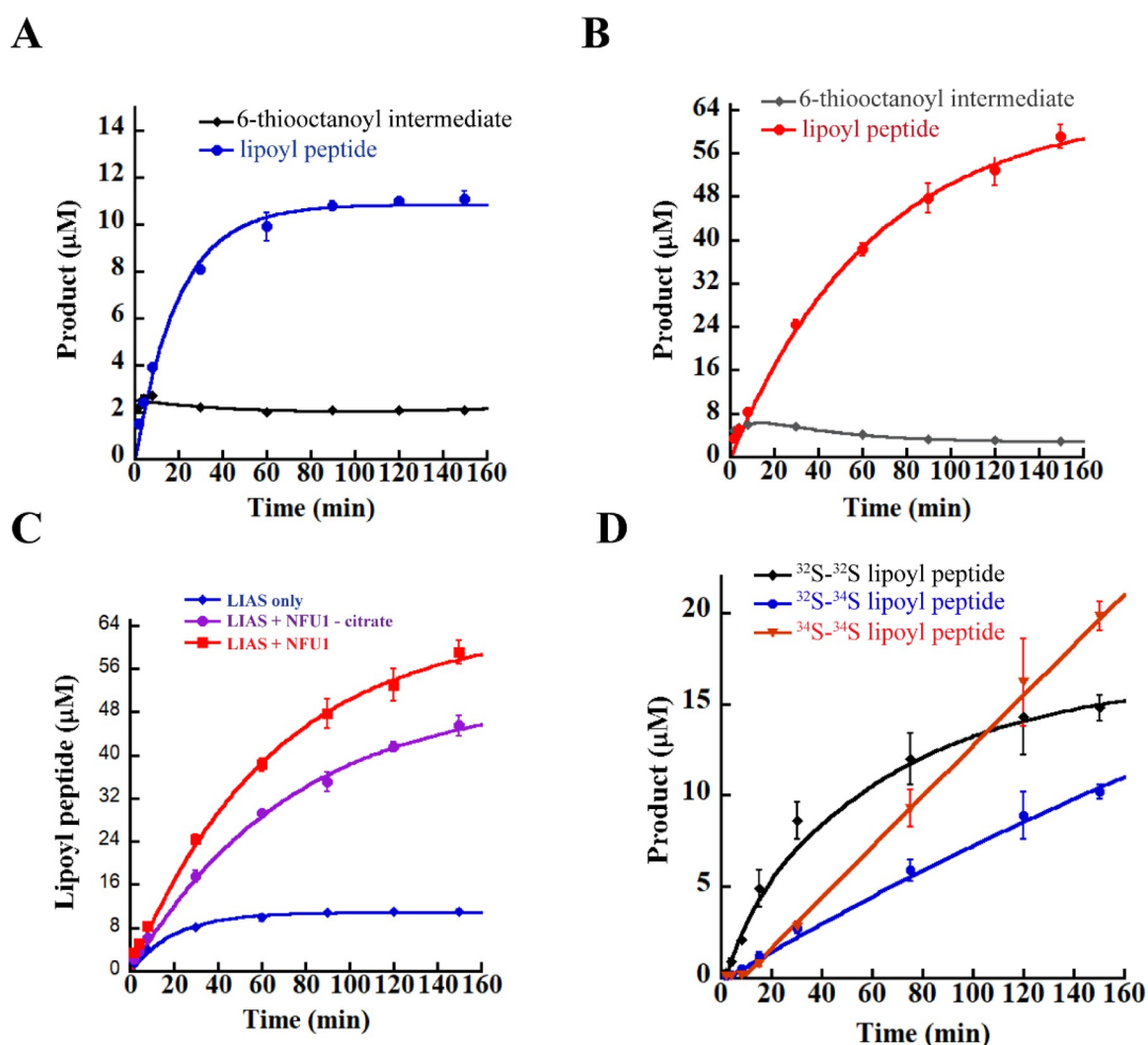


Figure 7. LIAS activity determinations: LIAS (10 μM) activity in the absence of NFU1 (A), in the presence of 200 μM NFU1 (B), in the presence of both 200 μM NFU1 and 5 mM sodium citrate (C), and in the presence of 200 μM NFU1 reconstituted with ^{34}S -labeled sulfide (D). LIAS alone catalyzes about 1 turnover of lipoyl product (blue trace) with the 6-thiooctanoyl intermediate quickly reaching a steady level (black trace) (A). The inclusion of an excess of NFU1 in the LIAS reaction promotes multiple turnovers and generation of more than 5 equiv of lipoyl product (red trace), while the formation and decay of the intermediate mimics that of LIAS alone (gray trace) (B). The inclusion of 5 mM sodium citrate, a divalent metal chelator, does not significantly alter the effect of NFU1 (purple trace) compared to reactions in which citrate is omitted (red trace) (C). In the presence of NFU1 reconstituted with $^{34}\text{S}^{2-}$, the ^{32}S -labeled lipoyl peptide product is formed first before formation of the mixed ^{32}S - ^{34}S (blue trace) and ^{34}S - ^{34}S -labeled (red trace) lipoyl peptide products (D). The data in panels C and D suggest direct cluster transfer from NFU1 to LIAS during turnover. Unless otherwise noted, all activity assays included the following at their indicated final concentrations: 350 μM octanoyl peptide substrate, 0.75 mM SAM, and 10 μM SAH nucleosidase. The reactions were carried out at room temperature in a buffer that contained 50 mM HEPES, pH 7.5, and 0.25 M KCl and were initiated with a final concentration of 1 mM dithionite. The respective data shown in panels A–D are averages from assays done in triplicate, and the error bars represent one standard deviation from the mean. The 6-thiooctanoyl intermediate data were fit to an exponential equation that accounts for its formation and decay phases (A and B), while the lipoyl peptide product data were fit to a biphasic double-exponential rate of formation equation, assuming an $\text{A} \rightarrow \text{B} \rightarrow \text{C}$ model, as has been previously reported for *M. tuberculosis* LipA (ref 72).

NFU1 Binds Tightly to LIAS

Our previous studies indicated that *E. coli* NfuA binds tightly to *E. coli* LipA, suggesting that NFU1 might interact similarly with LIAS, as has been determined recently through yeast two-hybrid analysis.⁷⁵ To assess whether NFU1 and LIAS form a tight complex in vitro, the holo (Fe–S cluster containing) forms of the two proteins were analyzed separately and together by SEC (Figure 6A). LIAS alone (blue trace) elutes at 62.5 mL, exhibiting an experimentally calculated mass of 46 kDa (theoretical mass, 39.2 kDa) based on the elution profiles of a suite of standards. NFU1 alone (black trace) elutes at 67.7

mL, exhibiting an experimentally calculated mass of 29.8 kDa (theoretical mass, 22 kDa). The sample containing both LIAS and NFU1 (red trace) shows an elution volume of 59.1 mL, corresponding to an experimentally calculated mass of 61.2 kDa, suggestive of a 1:1 heterodimer of LIAS and NFU1 (theoretical mass, 61.2 kDa). To confirm the results obtained by SEC, we subjected fractions from the peaks observed in the LIAS alone, NFU1 alone, and LIAS plus NFU1 traces to SDS–PAGE (Figure 6B). As shown, the peak from the LIAS plus NFU1 sample (lane 3) contains both NFU1 and LIAS. In these experiments, NFU1 migrates as a monomer and interacts with LIAS as a monomer. We further characterized the

interactions between NFU1 and LIAS by determining the equilibrium binding dissociation constant (K_D) using isothermal titration calorimetry (ITC, Figure 6C). The results from ITC indicate a K_D value of $0.7 \pm 0.2 \mu\text{M}$, confirming the strong interaction.

In Vitro Determination of LIAS Activity

LIAS in vitro activity was determined in assays using a four amino acid peptide substrate mimic containing an octanoylsyl residue [Glu-(N⁶-octanoyl)Lys-Ala-Tyr], a shorter version of the eight amino acid peptide previously used in *E. coli* LipA^{36,47} and *M. tuberculosis* LipA⁷² assays. For reasons that we do not understand, this shorter 4-mer peptide affords more turnovers than the longer 8-mer peptide. As shown in Figure 7A, the protein catalyzes formation of no more than 1 equiv of lipoyl product (blue trace), with no significant accumulation of the 6-thiooctanoyl intermediate (black trace), consistent with previous studies of *E. coli* LipA that indicate that the auxiliary cluster gets degraded as a function of turnover and that both sulfurs are contributed by the same LIAS polypeptide.⁶⁸

In Vitro Determination of NFU1 Effect on LIAS Activity

After establishing that NFU1 binds tightly to LIAS, we assessed whether NFU1 affects LIAS activity. As shown in Figure 7A, LIAS produces not more than 1 equiv of product in the absence of NFU1. By contrast, in the presence of excess NFU1 (200 μM monomer), 10 μM LIAS catalyzes more than 5 turnovers in a time-dependent manner over 150 min (Figure 7B, red trace). The lack of a clear burst followed by a slower phase of product formation suggests that regeneration of LIAS's auxiliary cluster is not rate-limiting, similar to what was observed with *E. coli* LipA and NfuA.⁴⁷ The amount of observed lipoyl product is less than what would be expected, given that the NFU1 dimer is in a 10-fold excess. Currently, we attribute the leveling off of activity to aberrant chemistry during destruction of the auxiliary cluster and its subsequent reconstitution. We predict that a more physiological system, especially with respect to the choice of reductant, may enhance the extent of turnover. To confirm that cluster transfer from NFU1 to LIAS is largely direct rather than a result of release of iron and sulfide into solution, the effect of NFU1 on LIAS activity was probed in the presence of 5 mM sodium citrate. Under these conditions, citrate will sequester free iron liberated by NFU1 and prevent it from being used to reconstitute LIAS. The observation that the presence of 5 mM citrate shows no dramatic effect on overall lipoyl product formation (Figure 7C) suggests that the transfer is direct, consistent with the finding that NFU1 and LIAS form a complex. The somewhat reduced activity is attributed to the ability of citrate to remove the cluster from NFU1, as was observed previously in experiments conducted with *E. coli* IscU.⁴⁷ Direct cluster transfer was further assessed by performing LIAS activity assays in the presence of an NFU1 protein that was chemically reconstituted with ³⁴S²⁻ to yield NFU1 containing a [4Fe-4³⁴S] cluster. Results from these studies show relatively rapid formation of ³²S-³²S-containing lipoyl product, which is followed by slower production of ³²S-³⁴S-containing and ³⁴S-³⁴S-containing lipoyl product (Figure 7D). The formation of lipoyl product containing the mixed isotope (³²S-³⁴S) was also observed with the *E. coli* NfuA/LipA system, although larger amounts of this product are formed with NFU1/LIAS.⁴⁷ It is not clear whether mixed-isotope formation is due to the conditions of the assay (e.g., presence of dithionite or incomplete LIAS reconstitution) or is

intrinsic to how the cluster is transferred from NFU1/NfuA to LIAS/LipA. In reactions containing NfuA and LipA, almost 2 equiv of ³²S-³²S-containing lipoyl product was formed before formation of the ³⁴S-containing species. In the NFU1/LIAS reactions herein, it appears that almost 1.5 equiv of the ³²S-³²S-containing lipoyl product is formed during the reaction. These data suggest that potentially all four sulfides of the auxiliary cluster of LIAS can be used for lipoyl product formation. It should be noted that the total amount of lipoyl product generated when using ³⁴S-reconstituted NFU1 is lower than that when using NFU1 at natural abundance. We believe the difference is related to how each protein is produced. To generate ³⁴S-reconstituted NFU1, the protein is first isolated in its apo form before being reconstituted. By contrast, NFU1 at natural abundance is produced directly in its Fe-S cluster form, and then further reconstituted.

In Vitro Effect of NFU1 plus BOLA3 on LIAS Activity

Previous studies have implicated BOLA3 in lipoyl cofactor formation; however, it has not been established when exactly BOLA3 functions. BOLA3 is a mitochondrial Fe-S cluster assembly and trafficking factor that facilitates Fe-S cluster insertion into a subset of Fe-S cluster acceptor proteins, and it has been suggested that it might act synergistically with NFU1.⁸³ BOLA3 was previously reported to form heterodimeric complexes with NFU1 and also GLRX5, and its deletion was associated with defective lipoic acid biosynthesis in vivo, suggesting its requirement for LIAS Fe-S cluster maturation.^{65,83} With this precedent in mind, we tested whether BOLA3 could act synergistically with NFU1 for Fe-S cluster transfer to LIAS during turnover. However, inclusion of BOLA3 in our LIAS activity assays in the presence of NFU1 does not show any additional effect on turnover (Table 1 and Figure S3A). Moreover, SEC experiments similar to those conducted with LIAS and NFU1 show that BOLA3 does not bind tightly to LIAS.

In Vitro LIAS Activity Determination in the Presence of GLRX5, ISCA1, ISCA2, and ISCU

ISCA2 and ISCU have also been reported to be able to reconstitute LIAS, transforming an inactive protein into one that is competent for catalysis.⁷⁴ In other work, *E. coli* IscU was reported to reconstitute *E. coli* LipA, allowing for multiple

Table 1. Effect of Fe-S Cluster Assembly Proteins on LIAS Activity^a

NFU1	BOLA3	ISCA1	ISCA2	ISCU	GLRX5	effect on LIAS activity ^b
X						increase to 5–6 turnovers
X	X					same as NFU1 alone
		X				increase to ~1.5 turnovers
			X			increase to ~2 turnovers
				X		slight increase to ~1 turnover
					X	no observed effect
	X				X	no observed effect

^aX denotes the presence of that protein in reaction mixtures. ^bDue to differences in LIAS cluster content from batch to batch, the observed turnover numbers vary by about 10–20%. We present the best turnover numbers observed for each corresponding protein or protein mixture.

turnovers,⁴⁷ while in another study, ISCA1, ISCA2, and IBA57 have been implicated in late-stage [4Fe–4S] cluster maturation, including Fe–S clusters in LIAS.⁸⁴ On the basis of these studies, we explored the effect of including purified and appropriately reconstituted GLRX5, ISCA1, ISCA2, and ISCU proteins in LIAS activity assays. Additionally, the effect of BOLA3 in activity assays that also included GLRX5 was tested. In summary, when either ISCA1 or ISCA2 are included in LIAS activity assays, only a modest increase in turnover is observed, up to an additional ~0.5 and ~1 equiv for ISCA1 and ISCA2, respectively. No change in LIAS turnover is observed by inclusion of ISCU, GLRX5, or BOLA3 in the presence of GLRX5 (Table 1 and Figure S3, parts B and C).

DISCUSSION

LS reductively cleaves SAM to generate 5'-dA· that abstracts substrate hydrogen atoms to allow for sequential sulfur insertions to produce the lipoyl cofactor. During turnover, LS sacrifices its auxiliary [4Fe–4S] cluster as the source of the sulfur atoms incorporated into the product, a process that leads to degradation of the auxiliary cluster. Thus, the enzyme is rendered inactive after a single turnover in the absence of a system that can regenerate the auxiliary cluster either by repairing it or by fully replacing it. Fe–S clusters are essential in all domains of life and are involved in various cellular processes, including respiration, ribosome assembly, DNA repair, and the biosynthesis of key metabolites.^{85–88} Due to the complexity of ISC assembly, trafficking, and repair mechanisms *in vivo*, these processes are yet to be fully understood. Understanding these mechanisms in humans is vital because Fe–S clusters and their incorporation into proteins that require them are critical to many serious diseases.^{55,56,63,89–91} While recent *in vitro* attempts to characterize Fe–S cluster assembly and trafficking have been reported, the determination of which late-acting carriers mediate LIAS auxiliary cluster regeneration during catalytic turnover remains unresolved. Here, we have investigated the effects of select human mitochondrial Fe–S cluster carriers (BOLA3, ISCA1, ISCA2, ISCU, GLRX5, and NFU1) on LIAS auxiliary cluster reconstitution during turnover and demonstrate for the first time that, like its *E. coli* counterpart NfuA, human NFU1 can efficiently reconstitute human LIAS during turnover to promote catalytic activity. Further, we show that NFU1 interacts tightly with LIAS, corroborating a similar finding from previously reported yeast two-hybrid experiments.⁷⁵ By contrast, ISCA1 and ISCA2 only partially enhance turnover of LIAS. It is likely that ISCA1 and ISCA2 are involved in *de novo* Fe–S incorporation into LIAS and not incorporation during catalytic turnover. Moreover, our studies suggest that neither BOLA3, GLRX5, nor ISCU are involved in the immediate regeneration of the auxiliary cluster of LIAS during turnover, although it appears that ISCU, like ISCA1 and ISCA2, can reconstitute LIAS *de novo*. Our studies suggest that the mechanism by which NFU1 transfers its cluster to LIAS during turnover is distinct from *de novo* reconstitution of LIAS and provide the basis for an additional system on which to investigate this transfer.

MATERIALS AND METHODS

Materials

N-(2-Hydroxyethyl)-piperazine-*N'*-(2-ethanesulfonic acid) (HEPES) was purchased from Fisher Scientific. Imidazole was purchased from J.

T. Baker Chemical Co. Potassium chloride and glycerol were purchased from EMD Chemicals. 2-Mercaptoethanol (BME), sodium dithionite, phenylmethylsulfonyl fluoride (PMSF), pyridoxal 5'-phosphate (PLP), and sodium sulfide were purchased from MilliporeSigma. Dithiothreitol (DTT), tris(2-carboxyethyl)phosphine hydrochloride (TCEP-HCl), kanamycin, ampicillin, arabinose, and isopropyl β -D-1-thiogalactopyranoside (IPTG) were purchased from Gold Biotechnology. Nickel-nitrilotriacetic acid (Ni-NTA) resin was acquired from Qiagen. *S*-Adenosyl-L-methionine (SAM) was synthesized and purified as described previously.⁹² Restriction enzymes and materials for cloning were obtained from New England Biolabs (Ipswich, MA). DNA isolation kits were purchased from Macherey-Nagel (Dueren, Germany). All other chemicals and materials were of the highest grade available and were from MilliporeSigma.

All peptides used in this study were custom-synthesized by Proimmune (Oxford, U.K.) except the octanoyl-containing peptide substrate [Glu-(N⁶-octanoyl)Lys-Ala-Tyr], which was synthesized by Genscript (Piscataway, NJ, U.S.A.). AtsA peptide (Pro-Met-Ser-Ala-Pro-Ala-Arg-Ser-Met) was used as an external standard for quantification of peptide products during liquid chromatography–mass spectrometry (LC–MS) analysis. An 8-thiooctanoyl-containing peptide [Glu-(N⁶-8-thiooctanoyl)Lys-Ala-Tyr] and a lipoyl-containing peptide [Glu-(N⁶-lipoyl)Lys-Ala-Tyr] were used as product standards for the 6-thiooctanoyl intermediate and lipoyl products, respectively.

General Methods

UV–vis spectra were recorded on a Varian Cary 50 spectrometer (Walnut Creek, CA) using the WinUV software package to control the instrument. Ultraperformance liquid chromatography (UPLC) was conducted on an Agilent Technologies 1290 Infinity II system coupled to an Agilent Technologies 6470 QQQ mass spectrometer (Santa Clara, CA) with detection by tandem mass spectrometry (MS/MS). Data collection and analysis were performed using the associated MassHunter software package.

Plasmids and Strains

Genes encoding *Homo sapiens* BOLA3 (aa 27–107), ISCA1 (aa 13–129), ISCA2 (aa 9–154), ISCU (aa 35–167), GLRX5 (aa 32–157), LIAS (aa 28–372), and NFU1 (aa 59–254) without their respective mitochondrial targeting sequences were synthesized at ThermoFisher Scientific after codon optimization using GeneArt software (ThermoFisher Scientific) for protein overexpression in *E. coli*. The genes were subcloned into a modified pSUMO plasmid (LifeSensors Inc.), (pDWSUMO), and pET28a vectors using *Nde*I and either *Xho*I or *Bam*HI restriction sites. After sequence verification by DNA sequencing at the Penn State Genomics Core Facility (University Park, PA), the resulting plasmids, pDWSUMO-BOLA3, pDWSUMO-ISCA1, pDWSUMO-ISCA2, pDWSUMO-ISCO, pDWSUMO-GLRX5, pDWSUMO-LIAS, and pDWSUMO-NFU1 (and their corresponding pET28a counterparts), were separately used to transform *E. coli* BL21 (DE3) competent cells containing the pDB1282 plasmid, which harbors the *isc* operon from *A. vinelandii*.⁹³ As cloned, each of the proteins in the pDWSUMO plasmid was expressed as a fusion with an N-terminal SUMO tag that also contained a His₆-tag at the N-terminus, while their counterparts cloned in pET28a were expressed with an N-terminal His₆-tag. During purification, the SUMO tag was removed using ULP1 protease, affording corresponding pure proteins with a Gly-His appendage at the N-terminus.

Growth and Expression of BOLA3, ISCA1, ISCA2, ISCU, GLRX5, LIAS, and NFU1

All proteins were overexpressed in *E. coli* using the following general procedure with minor adjustments for BOLA3 since it is not an Fe–S carrier protein by itself. In a typical growth, a 200 mL starter culture containing 25 μ g/mL kanamycin (50 μ g/mL for BOLA3) and 50 μ g/mL ampicillin (no ampicillin was included for BOLA3) was inoculated with a single colony and incubated overnight at 37 °C with shaking at 250 rpm. A 25 mL aliquot of the starter culture was used to inoculate 4 L of M9 minimal medium containing appropriate

antibiotic(s) as above and incubated at 37 °C with shaking (180 rpm) until an optical density at 600 nm (OD_{600}) of 0.3 was reached. At OD_{600} 0.3, 0.2% (w/v) L-arabinose was added to induce the expression of genes on the pDB1282 plasmid (except for BOLA3). At $OD_{600} \sim 0.6$, 50 μM FeCl_3 and 100 μM L-cysteine were added (except for BOLA3), and the culture was cooled in ice-water for 1 h with occasional shaking. Protein expression was induced by adding IPTG to a concentration of 0.2 mM, and incubation was continued at 18 °C with shaking at 180 rpm for an additional 12 h. The cells were harvested at 4 °C by centrifugation at 6000g for 15 min, flash-frozen in liquid nitrogen, and stored under liquid nitrogen until needed.

Protein Purification of BOLA3, ISCA1, ISCA2, ISCU, GLRX5, LIAS, and NFU1

The purification of each of the proteins was performed in an anaerobic chamber containing <1 ppm of O_2 (Coy Laboratory products, Grass Lake, MI) by IMAC using the following general procedures with minor modifications for BOLA3. Cells were resuspended in 200 mL of lysis buffer (100 mM Tris-HCl, pH 8.0, 150 mM KCl, 10 mM imidazole, 10 mM BME, 10 mM MgCl_2). To the resuspended cells, the following were added at their indicated final concentrations: 0.25 mM FeCl_3 , 1 mM L-cysteine, 1 mM PLP, one SIGMAFAST protease inhibitor tablet, 1 mM PMSF, 0.5 mg/mL lysozyme, and 0.01 mg/mL DNase (no FeCl_3 , cysteine, or PLP was added to BOLA3 samples). The cells were disrupted by sonication with an ultrasonic cell disruptor (Branson Sonifier II "model W-250", Heinemann), and the lysates were clarified by centrifugation (4 °C, 45 000g, 1 h). The N-terminally His₆-tagged SUMO fusion protein was then purified by Ni-NTA affinity chromatography. The Ni-NTA column was pre-equilibrated with 150 mL of lysis buffer. After loading the supernatant onto the Ni-NTA column, the resin was washed with 200 mL of wash buffer (50 mM HEPES, pH 7.5, 300 mM KCl, 30 mM imidazole, 10% glycerol (v/v), and 10 mM BME). Protein elution from the Ni-NTA resin was performed with 100 mL of elution buffer (50 mM HEPES, pH 7.5, 250 mM KCl, 300 mM imidazole, 10% glycerol, and 10 mM BME). The eluted protein was exchanged into cleavage buffer (50 mM HEPES, pH 7.5, 250 mM KCl, 5% glycerol, 40 mM imidazole, and 10 mM BME) using a PD-10 column. ULP1 protease (50 μg /mg of protein to be cleaved) was added to the fusion protein to excise the His₆-SUMO tag from the protein of interest, and the reaction mixture was incubated on ice overnight. The following day, the protein sample was reloaded onto the Ni-NTA column pre-equilibrated in cleavage buffer, and the protein of interest was collected in the flow-through. The protein was concentrated to ~ 2.5 mL and buffer-exchanged into storage buffer (50 mM HEPES, pH 7.5, 250 mM KCl, 30% glycerol, 2.5 mM TCEP, and 10 mM BME) using a PD-10 column (GE Healthcare). For proteins expressed from pET28a plasmid, their purification followed the same steps as described above, omitting the ULP1 cleavage step. When needed, the proteins were purified further by SEC on a HiPrep 16/60 Sephacryl HR S-200 column (Cytiva) equilibrated in gel filtration buffer (50 mM HEPES, pH 7.5, 250 mM KCl, 10% glycerol, 2.5 mM TCEP, and 10 mM BME) at a flow rate of 0.5 mL/min.⁹³ The S-200 column was connected to an AKTA protein liquid chromatography system (Cytiva) in an anaerobic chamber. Fractions containing the target protein were identified by UV-vis absorption at 280 nm and were combined, concentrated, and buffer-exchanged into storage buffer using a PD-10 column.

Amino acid analysis for LIAS and NFU1 was performed by the UC Davis Proteomics Core and revealed that the Bradford method overestimates the protein concentration of LIAS by a factor of 1.6 and that of NFU1 by a factor of 1.1. The concentration of the protein was determined by Bradford method using appropriate correction factors as necessary and using bovine serum albumin (fraction V) as the standard.⁹⁴ The purified protein sample was aliquoted, flash-frozen in liquid N_2 , and stored under liquid nitrogen until needed. Protein homogeneity was judged by 12% SDS-PAGE and was determined to be $\geq 95\%$ pure. Colorimetric iron and sulfide analyses were conducted on the purified protein using the methods of Beinert.^{95–97}

Overexpression and Purification of ⁵⁷Fe-Labeled LIAS and NFU1 and Mössbauer Spectroscopy

To generate ⁵⁷Fe-labeled proteins for analysis by Mössbauer spectroscopy, LIAS and NFU1 proteins were overproduced as described above with the exception that they were supplemented with 50 μM ⁵⁷FeCl₃ instead of 50 μM FeCl_3 . The growth and purification procedures were essentially identical to those described above, with the exception that ⁵⁷FeCl₃ was also used for reconstitution during the lysis step. ⁵⁷FeCl₃ was prepared as previously described.⁹⁸

For analysis by Mössbauer spectroscopy, 380 μM ⁵⁷Fe-labeled LIAS or 860 μM NFU1 was loaded into Mössbauer cups and flash-frozen in liquid nitrogen. Mössbauer spectra were recorded on a spectrometer from SEECO (Edina, MN) equipped with a Janis SVT-400 variable-temperature cryostat. Isomer shifts are reported relative to the centroid of the spectrum of α -iron metal at room temperature. The external magnetic field was applied parallel to the direction of propagation of the γ radiation. The Mössbauer spectra were simulated using the WMOSS spectral analysis software from SEECO (www.wmoss.org, SEE Co., Edina, MN).

Overexpression and Purification of ³⁴S-Labeled NFU1

The expression of apo-NFU1 was as reported for *EcNfuA*.⁴⁷ The protein was purified as described above with the exception that no FeCl_3 or cysteine was added during the lysis step, as was done for the other proteins. The purified apo protein was chemically reconstituted with FeCl_3 and Na_2^{34}S in the same manner as was reported for *EcNfuA*.⁴⁷ The reconstituted NFU1 was centrifuged at 14 000g for 10 min to remove aggregates, concentrated to 2.5 mL, and buffer-exchanged into gel filtration buffer using a PD-10 column. The protein was then further purified on an S-200 SEC column as described above. The synthesis of Na_2^{34}S followed the procedures previously reported.⁴⁷

Electron Paramagnetic Resonance Spectroscopy Analysis of LIAS and NFU1

For analysis by EPR, 400 μM LIAS or NFU1 in storage buffer was prepared at 4 °C inside an anaerobic chamber. After a 15 min reduction with freshly prepared dithionite (4 mM final concentration), the samples were flash-frozen in cryogenic isopentane. Respective protein samples without dithionite were used as controls. Continuous-wave EPR spectra data were collected at 10 K with a microwave power of 10 mW and a modulation amplitude of 0.2 mT on a Magnetech 5000 X-band ESR spectrometer (Bruker) equipped with an ER 4102ST resonator. The temperature was controlled by an ER 4112-HV Oxford Instruments (Concord, MA) variable-temperature helium-151 flow cryostat.

Interaction between NFU1 and LIAS

Size-Exclusion Chromatography. The ability of NFU1 to interact with LIAS was investigated using size-exclusion gel filtration chromatography. To determine the association, 500 μL of each of the following protein samples was applied to a pre-equilibrated (gel filtration buffer) HiPrep 16/60 Sephacryl HR S-200 column (GE Healthcare) housed in a Coy anaerobic glovebox (<1 ppm of O_2) and chromatographed using a flow rate of 0.5 mL/min. The elution volumes (V_e) of the following protein samples were determined: 100 μM LIAS alone, 200 μM NFU1 alone, and a 1:1 mixture of 200 μM LIAS plus 200 μM NFU1. For the molecular weight standard calibration curve, four individual injections were chromatographed for the standards as follows: a mixture of 250 μL of cytochrome *c* at 2 mg/mL (12.4 kDa) plus 250 μL of β -amylase at 4 mg/mL (200 kDa); a mixture of 250 μL of carbonic anhydrase at 3 mg/mL (29 kDa) plus 250 μL of alcohol dehydrogenase at 5 mg/mL (150 kDa); 500 μL of bovine serum albumin (66 kDa); 500 μL of blue dextran (2000 kDa). The elution volume of blue dextran was used for the void volume of the column (V_0). The V_e of the standards was determined, and the calibration curve was plotted as the log of the molecular mass versus V_e/V_0 . The linear equation was then used to calculate the experimental molecular weight of each sample. The interaction was judged both by the calculated experimental size of each of the peaks as

well as by a shift in the V_e . The presence of both LIAS and NFU1 was confirmed by SDS–PAGE.

Isothermal Titration Calorimetry. ITC was employed to confirm the interaction between LIAS and NFU1 observed using the gel filtration method above and to determine the binding dissociation constant (K_D). The K_D by ITC was determined by 2 μ L injections of LIAS (150 μ M in the syringe) into a solution of NFU1 (19 μ M in the cell) at 27 °C using a MicroCal VP-ITC calorimeter (Malvern Pananalytical Ltd.) housed in an anaerobic chamber (<1 ppm of O_2). Prior to the binding experiment, protein samples were thoroughly exchanged into ITC buffer (0.1 M HEPES pH 7.5, 0.5 M KCl, 5% glycerol, and 2 mM TCEP) by gel filtration chromatography using a PD-10 column. Binding analysis was accompanied by a control experiment in which LIAS ligand (150 μ M) was titrated into the sample cell containing only the ITC buffer. Before the data were fit, the control raw data were subtracted from the corresponding raw titration data to account for the heat associated with ligand dilution. The corrected data were processed with the Origin 7 software package (Malvern Pananalytical Ltd.).

Liquid Chromatography–Mass Spectrometry Activity Assays

Activity measurements were conducted in a Coy anaerobic chamber. Each reaction mixture contained the following at their final concentrations (unless noted otherwise elsewhere): 50 mM HEPES, pH 7.5, 250 mM KCl, 10 μ M LIAS, 10 μ M SAH nucleosidase, 0.75 mM SAM, and 350 μ M octanoyllysyl-containing peptide substrate [Glu-(N^6 -octanoyl)Lys-Ala-Tyr]. In reactions designed to assess the effect of BOLA3, ISCA1, ISCA2, ISCU, GLRX5, or NFU1, 200 μ M (final concentration) of each protein was added individually or in combination as needed. For reactions in which GLRX5 was added, reduced glutathione was included to a final concentration of 1 mM. For reactions designed to test direct cluster transfer from NFU1 to LIAS during turnover, sodium citrate was included to final concentration of 5 mM. All reactions were initiated by the addition of 1 mM (final concentration) sodium dithionite, and 25 μ L aliquots were removed at various times and added to an equal volume of quench solution that contained 300 mM H_2SO_4 , 8 mM TCEP, and 10 μ M AtsA peptide external standard. The samples were centrifuged at 14 000g for 30 min to remove any precipitated proteins. The time-dependent formation of 6-thiooctanoyl intermediate and lipoyl peptide products was determined by UPLC–MS/MS using multiple reaction monitoring (MRM) (Table S3). The quenched assay mixture was separated on an Agilent Technologies Zorbax Extend-C18 column Rapid Resolution HT (4.6 mm \times 50 mm, 1.8 μ m particle size) equilibrated in 98% solvent A (0.1% formic acid, pH 2.6) and 2% solvent B (100% acetonitrile). A solvent gradient of 2–65% B was applied from 0.5 to 2.5 min, the solvent composition was maintained at 65% B for 0.5 min before being returned to 2% B in 1 min, and then was retained at 2% B for an additional 1 min to re-equilibrate the column. A flow rate of 0.3 mL/min was maintained throughout the method (Table S4). The detection of the products was performed using electrospray ionization in positive mode (ESI⁺) with the following parameters: nitrogen gas temperature of 300 °C and flow rate of 5.0 L/min, nebulizer pressure of 15 psi, and capillary voltage of 4000 V. The products were quantified based on standard curves of product standards run under same conditions.

■ ASSOCIATED CONTENT

SI Supporting Information

The Supporting Information is available free of charge at <https://pubs.acs.org/doi/10.1021/acsbiochemau.2c00020>.

DNA and protein sequences, Mössbauer and EPR spectra, activity plots, and LC–MS conditions (PDF)

■ AUTHOR INFORMATION

Corresponding Authors

Squire J. Booker – Department of Chemistry, Biochemistry and Molecular Biology, and Howard Hughes Medical Institute, The Pennsylvania State University, University Park, Pennsylvania 16802, United States; orcid.org/0000-0002-7211-5937; Email: sjb14@psu.edu

Carsten Krebs – Department of Chemistry and Biochemistry and Molecular Biology, The Pennsylvania State University, University Park, Pennsylvania 16802, United States; orcid.org/0000-0002-3302-7053; Email: ckrebs@psu.edu

Authors

Douglas M. Warui – Department of Chemistry, The Pennsylvania State University, University Park, Pennsylvania 16802, United States; orcid.org/0000-0001-8950-9433

Debangsu Sil – Department of Chemistry, The Pennsylvania State University, University Park, Pennsylvania 16802, United States; orcid.org/0000-0002-0718-3925

Kyung-Hoon Lee – Department of Chemistry, The Pennsylvania State University, University Park, Pennsylvania 16802, United States

Syam Sundar Neti – Department of Chemistry, The Pennsylvania State University, University Park, Pennsylvania 16802, United States

Olga A. Esakova – Department of Chemistry, The Pennsylvania State University, University Park, Pennsylvania 16802, United States; orcid.org/0000-0001-8377-8368

Hayley L. Knox – Department of Chemistry and Biochemistry and Molecular Biology, Howard Hughes Medical Institute, The Pennsylvania State University, University Park, Pennsylvania 16802, United States

Complete contact information is available at:

<https://pubs.acs.org/doi/10.1021/acsbiochemau.2c00020>

Notes

The authors declare no competing financial interest.

■ ACKNOWLEDGMENTS

This work was supported by grants from the National Institutes of Health (awards GM-122595 to S.J.B. and GM-127079 to C.K.), the National Science Foundation (MCB-1716686 to S.J.B.), and the Eberly Family Distinguished Chair in Science (to S.J.B.). S.J.B. is an investigator of the Howard Hughes Medical Institute. This article is subject to HHMI's Open Access to Publications policy. HHMI lab heads have previously granted a nonexclusive CC BY 4.0 license to the public and a sublicensable license to HHMI in their research articles. Pursuant to those licenses, the author-accepted manuscript of this article can be made freely available under a CC BY 4.0 license immediately upon publication.

■ REFERENCES

- (1) Patterson, E. L.; et al. Crystallization of a Derivative of Protogenin B. *J. Am. Chem. Soc.* **1951**, *73* (12), 5919–5920.
- (2) Reed, L. J.; et al. Crystalline α -Lipoic Acid: A Catalytic Agent Associated with Pyruvate Dehydrogenase. *Science* **1951**, *114* (2952), 93.
- (3) Reed, L. *Advances in Enzymology and Related Areas of Molecular Biology*; John Wiley & Sons, Inc.: Hoboken, NJ, 2006; pp 319–347.

- (4) Fujiwara, K.; Okamura-Ikeda, K.; Motokawa, Y. Lipoylation of acyltransferase components of α -ketoacid dehydrogenase complexes. *J. Biol. Chem.* **1996**, *271*, 12932–12936.
- (5) Kang, S. G.; Jeong, H. K.; Lee, E.; Natarajan, S. Characterization of a lipoyl-transferase A gene of rice (*Oryza sativa* L.). *Gene* **2007**, *393* (1–2), 53–61.
- (6) Schonauer, M. S.; Kastaniotis, A. J.; Kursu, V. A.; Hiltunen, J. K.; Dieckmann, C. L. Lipoyl synthesis and attachment in yeast mitochondria. *J. Biol. Chem.* **2009**, *284*, 23234–23242.
- (7) Spalding, M. D.; Prigge, S. T. Lipoyl acid metabolism in microbial pathogens. *Microbiology and molecular biology reviews: MMBR* **2010**, *74* (2), 200–228.
- (8) Cronan, J. E. Biotin and Lipoyl Acid: Synthesis, Attachment, and Regulation. *EcoSal Plus* **2014**, *6* (1), 0001–2012.
- (9) Ewald, R.; et al. Lipoyl-Protein Ligase and Octanoyltransferase Are Essential for Protein Lipoylation in Mitochondria of Arabidopsis. *Plant Physiology* **2014**, *165* (3), 978–990.
- (10) Cronan, J. E. Assembly of lipoyl acid on its cognate enzymes: an extraordinary and essential biosynthetic pathway. *Microbiol. Mol. Biol. Rev.* **2016**, *80*, 429–450.
- (11) Solmonson, A.; DeBerardinis, R. J. Lipoyl acid metabolism and mitochondrial redox regulation. *J. Biol. Chem.* **2018**, *293*, 7522–7530.
- (12) Reed, L. J. A trail of research from lipoyl acid to -keto acid dehydrogenase complexes. *J. Biol. Chem.* **2001**, *276*, 38329–38336.
- (13) Mayr, J. A.; Feichtinger, R. G.; Tort, F.; Ribes, A.; Sperl, W. Lipoyl acid biosynthesis defects. *J. Inher. Metab. Dis.* **2014**, *37* (4), 553–563.
- (14) Habarou, F.; Hamel, Y.; Haack, T. B.; Feichtinger, R. G.; Lebigot, E.; Marquardt, et al. Biallelic mutations in LIPT2 cause a mitochondrial lipoylation defect associated with severe neonatal encephalopathy. *Am. J. Hum. Genet.* **2017**, *101*, 283–290.
- (15) Cao, X.; Zhu, L.; Song, X.; Hu, Z.; Cronan, J. E. Protein moonlighting elucidates the essential human pathway catalyzing lipoyl acid assembly on its cognate enzymes. *Proc. Natl. Acad. Sci. U. S. A.* **2018**, *115* (30), E7063–E7072.
- (16) Parry, R. J. Biosynthesis of lipoyl acid. 1. Incorporation of specifically tritiated octanoic acid into lipoyl acid. *J. Am. Chem. Soc.* **1977**, *99* (19), 6464–6466.
- (17) White, R. H. Stable isotope studies on the biosynthesis of lipoyl acid in *Escherichia coli*. *Biochemistry* **1980**, *19* (1), 15–19.
- (18) Jordan, S. W.; Cronan, J. E., Jr. A new metabolic link. *J. Biol. Chem.* **1997**, *272*, 17903–17906.
- (19) Jordan, S. W.; Cronan, J. E. [19] Biosynthesis of lipoyl acid and posttranslational modification with lipoyl acid in *Escherichia coli*. *Methods Enzymol.* **1997**, *279*, 176–183.
- (20) Jordan, S. W.; Cronan, J. E. The *Escherichia coli* lipB Gene Encodes Lipoyl (Octanoyl)-Acyl Carrier Protein:Protein Transferase. *J. Bacteriol.* **2003**, *185* (5), 1582–1589.
- (21) Nesbitt, N. M.; et al. Expression, purification, and physical characterization of *Escherichia coli* lipoyl(octanoyl)transferase. *Protein Expr Purif* **2005**, *39* (2), 269–82.
- (22) Parry, R. J.; Trainor, D. A. Biosynthesis of lipoyl acid. 2. Stereochemistry of sulfur introduction at C-6 of octanoic acid. *J. Am. Chem. Soc.* **1978**, *100* (16), 5243–5244.
- (23) Reed, K. E.; Cronan, J. E. Lipoyl acid metabolism in *Escherichia coli*: sequencing and functional characterization of the lipA and lipB genes. *J. Bacteriol.* **1993**, *175* (5), 1325–1336.
- (24) Miller, J. R.; et al. *Escherichia coli* LipA is a lipoyl synthase: in vitro biosynthesis of lipoylated pyruvate dehydrogenase complex from octanoyl-acyl carrier protein. *Biochemistry* **2000**, *39*, 15166–15178.
- (25) Cicchillo, R. M.; et al. Lipoyl synthase requires two equivalents of S-adenosyl-L-methionine to synthesize one equivalent of lipoyl acid. *Biochemistry* **2004**, *43* (21), 6378–86.
- (26) Oberg, N.; et al. RadicalSAM.org: A Resource to Interpret Sequence-Function Space and Discover New Radical SAM Enzyme Chemistry. *ACS Bio & Med Chem Au* **2022**, *2* (1), 22–35.
- (27) Broderick, J. B.; et al. Radical S-Adenosylmethionine Enzymes. *Chem. Rev.* **2014**, *114* (8), 4229–4317.
- (28) Landgraf, B. J.; McCarthy, E. L.; Booker, S. J. Radical S-Adenosylmethionine Enzymes in Human Health and Disease. *Annu. Rev. Biochem.* **2016**, *85* (1), 485–514.
- (29) Holliday, G. L.; et al. Atlas of the Radical SAM Superfamily: Divergent Evolution of Function Using a “Plug and Play” Domain. *Methods Enzymol* **2018**, *606*, 1–71.
- (30) Booker, S. J.; Grove, T. L. Mechanistic and functional versatility of radical SAM enzymes. *F1000 Biol. Rep.* **2010**, *2*, S2.
- (31) Bandarian, V. Journey on the Radical SAM Road as an Accidental Pilgrim. *ACS Bio Med Chem Au* **2022**.
- (32) Frey, P. A.; Booker, S. J. Radical mechanisms of S-adenosylmethionine-dependent enzymes. *Adv. Protein Chem.* **2001**, *58*, 1–45.
- (33) Frey, P. A.; Hegeman, A. D.; Ruzicka, F. J. The Radical SAM Superfamily. *Crit. Rev. Biochem. Mol. Biol.* **2008**, *43* (1), 63–88.
- (34) Cicchillo, R. M.; et al. *Escherichia coli* lipoyl synthase binds two distinct [4Fe–4S] clusters per polypeptide. *Biochemistry* **2004**, *43*, 11770–11781.
- (35) Douglas, P.; et al. Lipoyl synthase inserts sulfur atoms into an octanoyl substrate in a stepwise manner. *Angew. Chem., Int. Ed. Engl.* **2006**, *45* (31), 5197–9.
- (36) Lanz, N. D.; et al. Evidence for a catalytically and kinetically competent enzyme-substrate cross-linked intermediate in catalysis by lipoyl synthase. *Biochemistry* **2014**, *53*, 4557–4572.
- (37) Lanz, N. D.; et al. Characterization of a radical intermediate in lipoyl cofactor biosynthesis. *J. Am. Chem. Soc.* **2015**, *137*, 13216–13219.
- (38) Lanz, N. D.; Booker, S. J. Auxiliary iron-sulfur cofactors in radical SAM enzymes. *Biochim. Biophys. Acta* **2015**, *1853* (6), 1316–34.
- (39) Lanz, N. D.; Booker, S. J. The role of iron-sulfur clusters in the biosynthesis of the lipoyl cofactor. In *Iron-Sulfur Clusters in Chemistry and Biology*; Rouault, T. A., Ed.; Walter de Gruyter GmbH: Berlin, Germany, 2014.
- (40) Lanz, N. D.; Booker, S. J. Identification and function of auxiliary iron-sulfur clusters in radical SAM enzymes. *Biochim. Biophys. Acta* **2012**, *1824* (11), 1196–212.
- (41) Walsby, C. J.; et al. An anchoring role for FeS clusters: chelation of the amino acid moiety of S-adenosylmethionine to the unique iron site of the [4Fe–4S] cluster of pyruvate formate-lyase activating enzyme. *J. Am. Chem. Soc.* **2002**, *124*, 11270–11271.
- (42) Walsby, C. J.; et al. Electron-nuclear double resonance spectroscopic evidence that S-adenosylmethionine binds in contact with the catalytically active [4Fe–4S]⁺ cluster of pyruvate formate-lyase activating enzyme. *J. Am. Chem. Soc.* **2002**, *124*, 3143–3151.
- (43) Vey, J. L.; Drennan, C. L. Structural Insights into Radical Generation by the Radical SAM Superfamily. *Chem. Rev.* **2011**, *111* (4), 2487–2506.
- (44) Harmer, J. E.; et al. Structures of lipoyl synthase reveal a compact active site for controlling sequential sulfur insertion reactions. *Biochem. J.* **2014**, *464*, 123–133.
- (45) McLaughlin, M. I.; et al. Crystallographic snapshots of sulfur insertion by lipoyl synthase. *Proc. Natl. Acad. Sci. U. S. A.* **2016**, *113* (34), 9446–50.
- (46) McCarthy, E. L.; et al. The A-type domain in *Escherichia coli* NfuA is required for regenerating the auxiliary [4Fe–4S] cluster in *Escherichia coli* lipoyl synthase. *J. Biol. Chem.* **2019**, *294* (5), 1609–1617.
- (47) McCarthy, E. L.; Booker, S. J. Destruction and reformation of an iron-sulfur cluster during catalysis by lipoyl synthase. *Science* **2017**, *358* (6361), 373–377.
- (48) Maio, N.; Rouault, T. A. Iron-sulfur cluster biogenesis in mammalian cells: New insights into the molecular mechanisms of cluster delivery. *Biochim. Biophys. Acta* **2015**, *1853* (6), 1493–512.
- (49) Majewska, J.; et al. Binding of the Chaperone Jac1 Protein and Cysteine Desulfurase Nfs1 to the Iron-Sulfur Cluster Scaffold Isu Protein Is Mutually Exclusive. *J. Biol. Chem.* **2013**, *288* (40), 29134–29142.

- (50) Vickery, L. E.; Cupp-Vickery, J. R. Molecular chaperones HscA/Ssq1 and HscB/Jac1 and their roles in iron-sulfur protein maturation. *Crit Rev. Biochem Mol. Biol.* **2007**, *42* (2), 95–111.
- (51) Fox, N. G.; et al. The Human Iron-Sulfur Assembly Complex Catalyzes the Synthesis of [2Fe-2S] Clusters on ISCU2 That Can Be Transferred to Acceptor Molecules. *Biochemistry* **2015**, *54* (25), 3871–9.
- (52) Braymer, J. J.; Lill, R. Iron-sulfur cluster biogenesis and trafficking in mitochondria. *J. Biol. Chem.* **2017**, *292* (31), 12754–12763.
- (53) Braymer, J. J.; et al. Mechanistic concepts of iron-sulfur protein biogenesis in Biology. *Biochim Biophys Acta Mol. Cell Res.* **2021**, *1868* (1), 118863.
- (54) Pérard, J.; Ollagnier de Choudens, S. Iron–sulfur clusters biogenesis by the SUF machinery: close to the molecular mechanism understanding. *JBIC Journal of Biological Inorganic Chemistry* **2018**, *23* (4), 581–596.
- (55) Rouault, T. A.; Maio, N. Biogenesis and functions of mammalian iron-sulfur proteins in the regulation of iron homeostasis and pivotal metabolic pathways. *J. Biol. Chem.* **2017**, *292* (31), 12744–12753.
- (56) Rouault, T. A. Biogenesis of iron-sulfur clusters in mammalian cells: new insights and relevance to human disease. *Dis Model Mech* **2012**, *5* (2), 155–64.
- (57) Banci, L.; et al. [2Fe-2S] cluster transfer in iron–sulfur protein biogenesis. *Proc. Natl. Acad. Sci. U. S. A.* **2014**, *111* (17), 6203.
- (58) Nasta, V.; et al. A pathway for assembling [4Fe-4S](2+) clusters in mitochondrial iron-sulfur protein biogenesis. *Febs j* **2020**, *287* (11), 2312–2327.
- (59) Baker, P. R.; Friederich, M. W.; Swanson, M. A.; Shaikh, T.; Bhattacharya, K.; Scharer, G. H.; Aicher, J.; Creadon-Swindell, G.; Geiger, E.; MacLean, K. N.; et al. Variant non ketotic hyperglycinemia is caused by mutations in LIAS, BOLA3 and the novel gene GLRX5. *Brain* **2014**, *137* (2), 366–379.
- (60) Maio, N.; Jain, A.; Rouault, T. A. Mammalian iron-sulfur cluster biogenesis: Recent insights into the roles of frataxin, acyl carrier protein and ATPase-mediated transfer to recipient proteins. *Curr. Opin Chem. Biol.* **2020**, *55*, 34–44.
- (61) Ahting, U.; Mayr, J. A.; Vanlander, A. V.; Hardy, S. A.; Santra, S.; Makowski, C.; Alston, C. L.; Zimmermann, F. A.; Abela, L.; Plecko, B.; et al. Clinical, biochemical, and genetic spectrum of seven patients with NFU1 deficiency. *Front. Genet.* **2015**, *6*, 123.
- (62) Cameron, J.; et al. Mutations in Iron-Sulfur Cluster Scaffold Genes NFU1 and BOLA3 Cause a Fatal Deficiency of Multiple Respiratory Chain and 2-Oxoacid Dehydrogenase Enzymes. *American journal of human genetics* **2011**, *89*, 486–95.
- (63) Navarro-Sastre, A.; et al. A fatal mitochondrial disease is associated with defective NFU1 function in the maturation of a subset of mitochondrial Fe-S proteins. *Am. J. Hum. Genet.* **2011**, *89* (5), 656–67.
- (64) Wachnowsky, C.; et al. Understanding the Molecular Basis of Multiple Mitochondrial Dysfunctions Syndrome 1 (MMDS1)-Impact of a Disease-Causing Gly208Cys Substitution on Structure and Activity of NFU1 in the Fe/S Cluster Biosynthetic Pathway. *J. Mol. Biol.* **2017**, *429* (6), 790–807.
- (65) Melber, A.; Na, U.; Vashisht, A.; Weiler, B. D.; Lill, R.; Wohlschlegel, J. A.; Winge, D. R. Role of Nfu1 and Bol3 in iron-sulfur cluster transfer to mitochondrial clients. *Elife* **2016**, *5*, e15991.
- (66) Zhao, S.; et al. Assembly of the covalent linkage between lipoic acid and its cognate enzymes. *Chem. Biol.* **2003**, *10*, 1293–1302.
- (67) Billgren, E. S.; Cicchillo, R. M.; Nesbitt, N. M.; Booker, S. J. Lipoic acid biosynthesis and enzymology. In *Comprehensive Natural Products II Chemistry and Biology*; Mander, L., Liu, H.-W., Eds.; Elsevier: Oxford, U.K., 2010; pp 181–212.
- (68) Cicchillo, R. M.; Booker, S. J. Mechanistic investigations of lipoic acid biosynthesis in *Escherichia coli*: both sulfur atoms in lipoic acid are contributed by the same lipoyl synthase polypeptide. *J. Am. Chem. Soc.* **2005**, *127*, 2860–2861.
- (69) Cicchillo, R. M.; et al. Lipoyl synthase requires two equivalents of S-adenosyl-L-methionine to synthesize one equivalent of lipoic acid. *Biochemistry* **2004**, *43*, 6378–6386.
- (70) Douglas, P.; et al. Lipoyl synthase inserts sulfur atoms into an octanoyl substrate in a stepwise manner. *Angew. Chem.* **2006**, *118*, 5321–5323.
- (71) McLaughlin, M. I.; et al. Crystallographic snapshots of sulfur insertion by lipoyl synthase. *Proc. Natl. Acad. Sci. U S A* **2016**, *113*, 9446–9450.
- (72) Lanz, N. D.; et al. Characterization of Lipoyl Synthase from *Mycobacterium tuberculosis*. *Biochemistry* **2016**, *55* (9), 1372–83.
- (73) Camponeschi, F.; et al. Paramagnetic (1)H NMR Spectroscopy to Investigate the Catalytic Mechanism of Radical S-Adenosylmethionine Enzymes. *J. Mol. Biol.* **2019**, *431* (22), 4514–4522.
- (74) Hendricks, A. L.; et al. Characterization and Reconstitution of Human Lipoyl Synthase (LIAS) Supports ISCA2 and ISCU as Primary Cluster Donors and an Ordered Mechanism of Cluster Assembly. *Int. J. Mol. Sci.* **2021**, *22* (4), 1598.
- (75) Jain, A.; et al. Assembly of the [4Fe-4S] cluster of NFU1 requires the coordinated donation of two [2Fe-2S] clusters from the scaffold proteins, ISCU2 and ISCA1. *Hum. Mol. Genet.* **2020**, *29* (19), 3165–3182.
- (76) Johnson, D. C.; Unciuleac, M.-C.; Dean, D. R. Controlled Expression and Functional Analysis of Iron-Sulfur Cluster Biosynthetic Components within *Azotobacter vinelandii*. *J. Bacteriol.* **2006**, *188* (21), 7551–7561.
- (77) Pandelia, M. E.; et al. Mössbauer spectroscopy of Fe/S proteins. *Biochim. Biophys. Acta - Molecular Cell Research* **2015**, *1853* (6), 1395–1405.
- (78) Cai, K.; et al. Structural/Functional Properties of Human NFU1, an Intermediate [4Fe-4S] Carrier in Human Mitochondrial Iron-Sulfur Cluster Biogenesis. *Structure* **2016**, *24* (12), 2080–2091.
- (79) Wachnowsky, C.; et al. Regulation of human Nfu activity in Fe-S cluster delivery-characterization of the interaction between Nfu and the HSPA9/Hsc20 chaperone complex. *Febs j* **2018**, *285* (2), 391–410.
- (80) Wesley, N. A.; Wachnowsky, C.; Fidai, I.; Cowan, J. A.; et al. Understanding the molecular basis for multiple mitochondrial dysfunctions syndrome 1 (MMDS1): impact of a disease-causing Gly189Arg substitution on NFU1. *FEBS J.* **2017**, *284*, 3838–3848.
- (81) Jumper, J.; et al. Highly accurate protein structure prediction with AlphaFold. *Nature* **2021**, *596* (7873), 583–589.
- (82) Cai, K.; Frederick, R. O.; Markley, J. L. ISCU interacts with NFU1, and ISCU[4Fe-4S] transfers its Fe-S cluster to NFU1 leading to the production of holo-NFU1. *J. Struct Biol.* **2020**, *210* (2), 107491.
- (83) Uzarska, M. A.; Nasta, V.; Weiler, B. D.; Spantgar, F.; Ciofi-Baffoni, S.; Saviello, M. R.; Gonnelli, L.; Muhlenhoff, U.; Banci, L.; Lill, R. Mitochondrial Bol1 and Bol3 function as assembly factors for specific iron-sulfur proteins. *Elife* **2016**, *5*, e16673.
- (84) Sheftel, A. D.; et al. The human mitochondrial ISCA1, ISCA2, and IBA57 proteins are required for [4Fe-4S] protein maturation. *Mol. Biol. Cell* **2012**, *23* (7), 1157–66.
- (85) Beinert, H.; Holm, R. H.; Münck, E. Iron-sulfur clusters: nature's modular, multipurpose structures. *Science* **1997**, *277*, 653–659.
- (86) Johnson, M. K. Iron–Sulfur Proteins: New Roles for Old Clusters. *Curr. Opin. Chem. Biol.* **1998**, *2*, 173–181.
- (87) Honarmand Ebrahimi, K.; et al. Iron-sulfur clusters as inhibitors and catalysts of viral replication. *Nat. Chem.* **2022**, *14* (3), 253–266.
- (88) Pritts, J. D.; Michel, S. L. J. Fe-S clusters masquerading as zinc finger proteins. *J. Inorg. Biochem* **2022**, *230*, 111756.
- (89) Cameron, J. M.; Janer, A.; Levandovskiy, V.; MacKay, N.; Rouault, T. A.; Tong, W.-H.; Ogilvie, I.; Shoubridge, E. A.; Robinson, B. H.; et al. Mutations in iron-sulfur cluster scaffold genes NFU1 and BOLA3 cause a fatal deficiency of multiple respiratory chain and 2-oxoacid dehydrogenase enzymes. *Am. J. Hum. Genet.* **2011**, *89*, 486–495.
- (90) Lossos, A.; et al. Fe/S protein assembly gene IBA57 mutation causes hereditary spastic paraplegia. *Neurology* **2015**, *84* (7), 659–67.

(91) Debray, F. G.; et al. Mutation of the iron-sulfur cluster assembly gene IBA57 causes fatal infantile leukodystrophy. *J. Inherit Metab Dis* **2015**, *38* (6), 1147–53.

(92) Iwig, D. F.; Booker, S. J. Insight into the polar reactivity of the onium chalcogen analogues of S-adenosyl-L-methionine. *Biochemistry* **2004**, *43* (42), 13496–13509.

(93) Lanz, N. D.; et al. RlmN and AtsB as models for the overproduction and characterization of radical SAM proteins. *Methods Enzymol.* **2012**, *516*, 125–152.

(94) Bradford, M. A rapid and sensitive method for the quantitation of microgram quantities of protein utilizing the principle of protein dye-binding. *Anal. Biochem.* **1976**, *72*, 248–254.

(95) Beinert, H. Micro methods for the quantitative determination of iron and copper in biological material. *Methods Enzymol.* **1978**, *54*, 435–445.

(96) Beinert, H. Semi-micro methods for analysis of labile sulfide and of labile sulfide plus sulfane sulfur in unusually stable iron-sulfur proteins. *Anal. Biochem.* **1983**, *131*, 373–378.

(97) Kennedy, M. C.; et al. Evidence for the Formation of a Linear [3Fe-4S] Cluster in Partially Unfolded Aconitase. *J. Biol. Chem.* **1984**, *259* (23), 14463–14471.

(98) Blaszczyk, A. J.; et al. Spectroscopic and Electrochemical Characterization of the Iron-Sulfur and Cobalamin Cofactors of TsrM, an Unusual Radical S-Adenosylmethionine Methylase. *J. Am. Chem. Soc.* **2016**, *138* (10), 3416–3426.